Impact of diffusion on surface clustering in random hydrodynamic flows

V. I. Klyatskin*
A.M. Obukhov Atmospheric Physics Institute of RAS, 3, Pyzhevsky per., Moscow 119017, Russia

K. V. Koshel†
V.I. Il'ichev Pacific Oceanological Institute of RAS, 43, Baltiyskaya street, Vladivostok 690041, Russia
and Far Eastern Federal University 8, Sukhanova street, Vladivostok, Russia

(Received 23 August 2016; revised manuscript received 14 November 2016; published 17 January 2017; corrected 19 January 2017)

Buoyant material clustering in a stochastic flow, which is homogeneous and isotropic in space and stationary in time, is addressed. The dynamics of buoyant material in three-dimensional hydrodynamic flows can be considered as the motion of passive tracers in a compressible two-dimensional velocity field. The latter is of interest in the present study. It is well known that the clustering of the density of passive tracers occurs in this case. We evaluate the impact of diffusion on the clustering process by using a numerical model. In general, the effect of diffusion is negligible in the very beginning of the evolution of initially uniformly distributed passive tracers. Therefore, the clustering of the density of passive tracers can emerge in accordance with the general theory. We analyze the long time clustering affected by diffusion and show that the emerged cluster structure persists in time in spite of the diffusion effect. However, the clusters split in time.

DOI: 10.1103/PhysRevE.95.013109

I. INTRODUCTION

Studying the passive tracer motion in random hydrodynamic flows is important to get insight into a vast range of physical problems including impurities spreading in the ocean and atmosphere [1–3]. For instance, floating debris concentrated in garbage islands [4,5] or oil from seeps and spills converges in irregular clusters at the ocean surface [3]. It also plays a role in the oceanic ecosystems [1], in cloud dynamics [6], porous media [7], planetology [8], or the mass distribution in the Universe formation [9].

The case of compressible velocity fields attracts special interest since, on the one hand, they permit the appearance of cluster structures [10–14]. On the other hand, the dynamics of buoyant [15,16] and low-inertia impurities [17–19] in hydrodynamic flows can be considered as the motion of passive tracers in a compressible velocity field [20,21].

We use a Lagrangian method to simulate numerically the advection of floating tracers in random hydrodynamic flows to assess the diffusion effect for a long time [10,22]. Our approach is similar to the ones suggested in the works [23,24], but we consider a potential velocity field, which needs additional calculation of the divergence along material trajectories. It is the Lagrangian divergence that induces clustering [3,10,18].

The aim of our study is to determine the influence of diffusion on cluster structuring of material density of floaters for a long time evolution. In the problem of laser emission in random media, the appearance of cluster splitting under influence of diffraction, which acts as the diffusion in Schrödinger equation [18], was reported. In this work, we aim at finding an analogous effect for the problem of particle clustering. As mentioned above, the horizontal divergence that corresponds to compressibility in the surface flow leads to clustering. The scale of divergence in a rapidly varying velocity field can be smaller than the diffusion scale, and, therefore, one can observe clustering below the diffusion scale. It is worth noting that in an earlier work [22], a similar model was numerically studied. However, the resolution and time interval were insufficient to reveal the effect of the cluster splitting below the diffusion scale. Therefore, the present work presents evidence of the phenomenon using a fine resolution and longer calculation time.

In Sec. II, the problem formulation and statistical properties of the random velocity field model are described. In Sec. III, we give a brief review of statistical topography characteristics and relevant results for clustering in the absence of diffusion. In Sec. IV, we discuss a method for modeling a random velocity field numerically and for calculating the density of buoyant material over a long time. The numerical results are also discussed in this section. The conclusions are given in Sec. V.

II. FORMULATION OF THE PROBLEM

The Eulerian dynamics of a passive tracer material density field $\rho(\mathbf{r},t)$ advected by a velocity field $\mathbf{u}(\mathbf{r},t)$ is described by the following partial differential equation [25–27]:

$$\left(\frac{\partial}{\partial t}+\frac{\partial}{\partial \mathbf{r}}\mathbf{u}(\mathbf{r},t)\right)\rho(\mathbf{r},t)=\kappa\,\Delta\rho(\mathbf{r},t), \tag{1}$$

where $\rho(\mathbf{r},0)=\rho_0(\mathbf{r})$ is an initial condition. Here, κ is the diffusion coefficient, and stochastic properties of the equation followed from $\mathbf{u}(\mathbf{r},t)$ being a random velocity field with a given statistical features.

Let us consider the diffusion of a floating tracer following Refs. [15,18,28]. If a passive tracer moves with horizontal and vertical velocity components $\mathbf{u}=(\mathbf{U},w)$ over the surface $z=0$ in an incompressible medium $[div\,\mathbf{u}(\mathbf{r},t)=0]$ in the absence of a mean flow, then an effective compressible two-dimensional flow with two-dimensional divergence

$$\nabla_{\mathbf{R}}\mathbf{U}(\mathbf{R},t)=-\left.\frac{\partial w(\mathbf{r},t)}{\partial z}\right|_{z=0}$$

*klyatskin@yandex.ru
†kvkoshel@poi.dvo.ru

is created on the surface. Representing the floating tracer field as $\rho(\mathbf{r},t) = \rho(\mathbf{R},t)\delta(z)$ and substituting this expression into (1), and then integrating with respect to z leads to the equation

$$\left(\frac{\partial}{\partial t} + \frac{\partial}{\partial \mathbf{R}}\mathbf{U}(\mathbf{R},t)\right)\rho(\mathbf{R},t) = \kappa\Delta_{\mathbf{R}}\rho(\mathbf{R},t). \tag{2}$$

As a result, we can consider a two-dimensional compressible random velocity field $\mathbf{U}(\mathbf{R},t)$. The dynamical system (2) is conservative with a constant mass of all the buoyant tracers $M = \int d\mathbf{R}\rho(\mathbf{R},t)$.

All the values involved are considered to be dimensionless with the space and time scales being L_0, t_0 and the tracer density scale being ρ^*. As a result, the characteristic size of a scalar patch in the dimensionless coordinates is of the order of 1, the initial tracer density is also of the order of 1, and t_0 is chosen to be equal to the discretization step since we assume that the velocity field is δ correlated in time. The velocity scale is then L_0/t_0, and the diffusivity scale is L_0^2/t_0.

A special feature of the equation (2) in the case of compressible flows is that the density field $\rho(\mathbf{R},t)$ is parametrically excited in every realization in time [10,13,14]. In the absence of the diffusion, the density field is governed by a first-order equation with partial derivatives [10]. Every realization of the corresponding velocity fields may produce clusters, i.e., there may appear compact regions with high values of the material density of tracers and with significantly lower background values. It is worth noticing that the quantities averaged over velocity field realizations do not bear any information on the emerging clusters. The stochastic structure formation in space in specific realizations of the random velocity field is of interest. This problem can be tackled by means of analyzing the one-point probability density of the solution. Various functions of the moments of the density fields for the equation in question are considered in many papers (see, for example, Refs. [13,14]). In particular, as the cluster formation triggers, all the functions of the moments of the density field exponentially grow in time in any particular point in space.

A. Statistical characteristics of a random velocity field

Let the random velocity field $\mathbf{U}(\mathbf{R},t)$ be potential, two-dimensional, Gaussian with zero mean, statistically homogeneous and isotropic in space, and statistically stationary in time. Thus, correlation and spectral functions are

$$\begin{aligned} B_{\alpha\beta}(\mathbf{R}',\eta) &= \langle U_\alpha(\mathbf{R},t)U_\beta(\mathbf{R}+\mathbf{R}',t+\eta)\rangle \\ &= \int d\mathbf{k}E(k,\eta)\frac{k_\alpha k_\beta}{k^2}e^{i\mathbf{k}\mathbf{R}'}. \end{aligned} \tag{3}$$

Let $B_{\alpha\beta}(\mathbf{0},0) = \langle U_\alpha(\mathbf{R},t)U_\beta(\mathbf{R},t)\rangle = \frac{1}{2}\sigma_{\mathbf{U}}^2\delta_{\alpha\beta}$, and the velocity field variance is

$$\sigma_{\mathbf{U}}^2 = B_{\alpha\alpha}(\mathbf{0},0) = \int d\mathbf{k}E(k,0).$$

Let us introduce the effective diffusion coefficient appeared due to random velocity field

$$\begin{aligned} D &= \int_0^\infty d\eta \int d\mathbf{k}\,k^2E(k,\eta) \\ &= \int_0^\infty d\eta\left\langle\frac{\partial\mathbf{U}(\mathbf{R},t+\eta)}{\partial\mathbf{R}}\frac{\partial\mathbf{U}(\mathbf{R},t)}{\partial\mathbf{R}}\right\rangle, \end{aligned} \tag{4}$$

where $\partial\mathbf{U}(\mathbf{R},t)/\partial\mathbf{R}$ is the velocity field divergence. The coefficient D from (4) can be expressed through the statistical parameters of the derivatives of the velocity field

$$D = \sigma_{div\mathbf{U}}^2\tau_{div\mathbf{U}},$$

where $\sigma_{div\mathbf{U}}$ and $\tau_{div\mathbf{U}}$ are variance and correlation time of velocity field divergence [14]. Now, to get insight into the space clustering of the random field $\rho(\mathbf{R},t)$ in almost every realization, we employ the ideas of statistical topography [13,14].

III. STATISTICAL TOPOGRAPHY OF RANDOM FIELDS

At any fixed point in the space $\tilde{\mathbf{R}}$, function $\rho(\tilde{\mathbf{R}},t)$ is a random process in time with the simultaneous probability density independent of $\tilde{\mathbf{R}}$. In the physical space $\{\mathbf{R}\}$, there may appear a structure in the field $\rho(\mathbf{R},t)$ as a physical object. These structures appear as closed regions with a high tracer concentration, conventionally called clusters.

Let us consider the diffusion of the density field $\rho(\mathbf{r},t)$ in a random velocity field at the initial stage. The stochastic clustering is governed by Eq. (2) at $\kappa = 0$. In the case of the one-point probability density, one can formulate an equation [13,14,18] with a solution corresponding to the log-normal process

$$P(t;\rho) = \frac{1}{2\rho\sqrt{\pi t/\tau}}\exp\left\{-\frac{\ln^2(\rho e^{t/\tau}/\rho_0)}{4t/\tau}\right\}, \tag{5}$$

where $\tau = 1/D$ is the effective diffusion dimensionless time scale. The corresponding integral distribution function is

$$\Phi(t;\rho) = \int_0^\rho d\rho' P(t;\rho') = \Pr\left(\frac{\ln(\rho e^{t/\tau}/\rho_0)}{2\sqrt{t/\tau}}\right), \tag{6}$$

where the function $\Pr(z)$ is the probability integral,

$$\Pr(z) = \frac{1}{\sqrt{2\pi}}\int_{-\infty}^z dx\exp\left\{-\frac{x^2}{2}\right\}.$$

We can now analyze the clustering of floaters from the statistical topography [13,14,29] point of view. We introduce the indicator function

$$\varphi(\mathbf{R},t;\rho) = \delta(\rho(\mathbf{R},t)-\rho).$$

With the help of this function, one can assess, for instance, the area of the regions with the random field $\rho(\mathbf{R},t)$ exceeding a prescribed level ρ, i.e., $\rho(\mathbf{R},t) > \rho$:

$$S(t;\rho) = \int d\mathbf{R}\,\theta(\rho(\mathbf{R},t)-\rho) = \int d\mathbf{R}\int_\rho^\infty d\rho'\,\varphi(\mathbf{R},t;\rho')$$

with the total mass of the tracers, encompassed in the areas

$$\begin{aligned} M(t;\rho) &= \int d\mathbf{R}\,\rho(\mathbf{R},t)\theta[\rho(\mathbf{R},t)-\rho] \\ &= \int d\mathbf{R}\int_\rho^\infty d\rho'\,\rho'\varphi(\mathbf{R},t;\rho'), \end{aligned}$$

where $\theta[\rho(\mathbf{R},t)-\rho]$ is the Heaviside step function.

The mean value of the indicator function averaged over the realization ensemble of the random velocity field determines the probability density $P(\mathbf{R},t;\rho) = \langle\delta[\rho(\mathbf{R},t)-\rho]\rangle$ simultaneous in time and one-point in space [13,14]. Therefore,

the mean values averaged over the random velocity field realization ensemble of $S(t;\rho)$ and $M(t;\rho)$ ensue as follows

$$\langle S(t;\rho)\rangle = \int d\mathbf{R}\int_{\rho}^{\infty} d\rho'\, P(\mathbf{R},t;\rho'),$$

$$\langle M(t;\rho)\rangle = \int d\mathbf{R}\int_{\rho}^{\infty} d\rho'\, \rho' P(\mathbf{R},t;\rho').$$

In the case of a field $\rho(\mathbf{R},t)$ homogeneous in space, the one-point probability density $P(\mathbf{R},t;\rho)$ is independent of $\mathbf{R}$. Therefore, the statistical means of the relations describe specific (related to the unit area) values of the corresponding quantities.

Hence, the specific mean area $\langle s_{\rm hom}(t;\rho)\rangle$, with the random field $\rho(\mathbf{R},t)$ exceeding the prescribed level ρ, coincides with the probability of the event occurrence $\rho(\mathbf{R},t) > \rho$ in every point in the space

$$\langle s_{\rm hom}(t;\rho)\rangle = \langle\theta[\rho(\mathbf{R},t)-\rho]\rangle = \mathrm{P}\{\rho(\mathbf{R},t) > \rho\} = \int_{\rho}^{\infty} d\rho' \mathrm{P}(t;\rho').$$

This is also a geometrical interpretation of the probability of the event occurrence $\rho(\mathbf{R},t) > \rho$ independent of the point $\mathbf{R}$. The specific mean mass of tracers encompassed in the areas $s_{\rm hom}(t;\rho)$ is defined as

$$\langle m_{\rm hom}(t;\rho)\rangle = \int_{\rho}^{\infty} d\rho'\, \rho' P(t;\rho').$$

In the case of a positive definite field $\rho(\mathbf{R},t)$, the condition of clustering with probability 1, i.e., in almost every realization, results from the asymptotic relations being simultaneously satisfied as $t \to \infty$. The asymptotic relations in the homogeneous case are [13,14]

$$\langle s_{\rm hom}(t;\rho)\rangle \to 0, \quad \langle m_{\rm hom}(t;\rho)\rangle \to \langle\rho(t)\rangle.$$

Thus, in the case of a potential flow, the density field always clusters with probability 1. For the mean specific area with $\rho(\mathbf{r},t) > \bar\rho$ it follows from (5)

$$\langle s_{\rm hom}(t,\bar\rho)\rangle = \mathrm{Pr}\left(\frac{\ln(\rho_0\, e^{-t/\tau}/\bar\rho)}{\sqrt{2t/\tau}}\right), \tag{7}$$

and the specific mass of the impurity concentrated in the area is

$$\langle m_{\rm hom}(t,\bar\rho)\rangle = \rho_0\,\mathrm{Pr}\left(\frac{\ln(\rho_0\, e^{t/\tau}/\bar\rho)}{\sqrt{2t/\tau}}\right). \tag{8}$$

From (7), (8), it follows that given $\tau \gg 1$, the mean specific area decreases according to the law

$$\langle s_{\rm hom}(t,\bar\rho)\rangle = \mathrm{P}\{\rho(\mathbf{R},t) > \bar\rho\} \approx \sqrt{\frac{\rho_0}{\pi\bar\rho t/\tau}}\, e^{-\frac{1}{4}\frac{t}{\tau}}, \tag{9}$$

while almost all the tracers concentrate inside this region

$$\langle m_{\rm hom}(t,\bar\rho)\rangle/\rho_0 \approx 1 - \sqrt{\frac{\bar\rho}{\pi\rho_0 t/\tau}}\, e^{-\frac{1}{4}\frac{t}{\tau}}. \tag{10}$$

It is this process that corresponds to the effect of the density field clustering in a random velocity field.

IV. NUMERICAL SIMULATION

A. Numerical simulation of random velocity field

In this paper, we study the clustering taking into account the effect of diffusion. The algorithm of the numerical modeling of a random velocity field δ correlated in time with the correlation tensor (3) is as follows. We use a spectral representation of the velocity fields [22,30,31]

$$U_\beta(\mathbf{R},t) = \sigma_{\mathbf{U}} \int d\mathbf{k}[a(k,t) + ib(k,t)]\frac{k_\beta}{k}\exp(i\mathbf{kR}), \tag{11}$$

where $a(k,t),b(k,t)$ are given random Gaussian fields δ correlated in time and over the wave vector with the parameters

$$\langle a(k,t)\rangle = \langle b(k,t)\rangle = \langle a(\mathbf{k},t)b(\mathbf{k}',t')\rangle = 0,$$

$$\langle a(\mathbf{k},t)a(\mathbf{k}',t')\rangle = \langle b(\mathbf{k},t)b(\mathbf{k}',t')\rangle = \frac{A}{2}E^N(k)\delta(\mathbf{k}-\mathbf{k}')\delta(t-t').$$

The velocity field (11) has the correlation tensor (3).

Further, one can represent the random fields $a(k,t),b(k,t)$ as discrete scalar Gaussian δ correlated processes with the variance $\sqrt{\frac{A}{2}E^N(k)}$. We use piecewise random functions constant in every discretization cell, and random Gaussian series with independent values. Instead of (11), we use a discrete analog of the Fourier transform. In our calculations, we use the spectral function

$$E^N = \frac{1}{2\pi}\frac{l^4}{4}k^2\exp\left\{-\frac{1}{2}k^2l^2\right\},$$

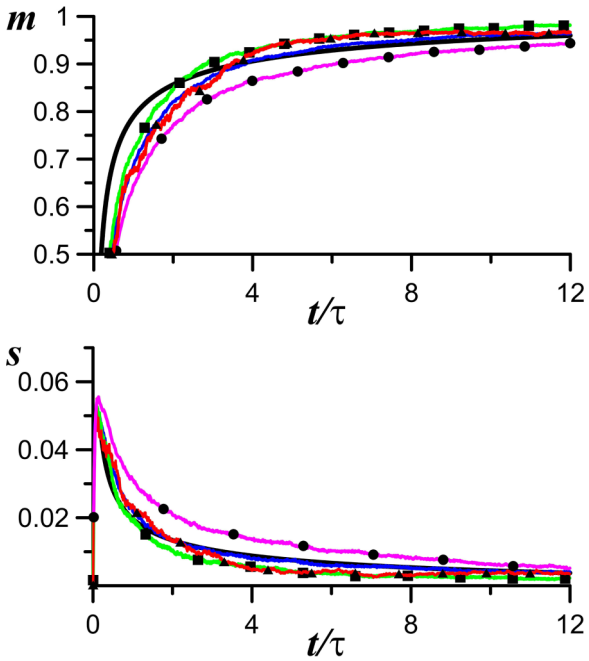

FIG. 1. A realization of the area and the mass of the clusters at $\bar\rho = 2.0$ for the parameters $l = 0.02, \sigma_{\mathbf{u}} = 0.166$, marked by circles (magenta); $l = 0.04, \sigma_{\mathbf{u}} = 0.333$, not marked (blue); $l = 0.08, \sigma_{\mathbf{u}} = 0.333$, marked by squares (green); $l = 0.16, \sigma_{\mathbf{u}} = 0.666$, marked by triangles (red). The bold lines indicate the asymptotic solutions (9), (10).

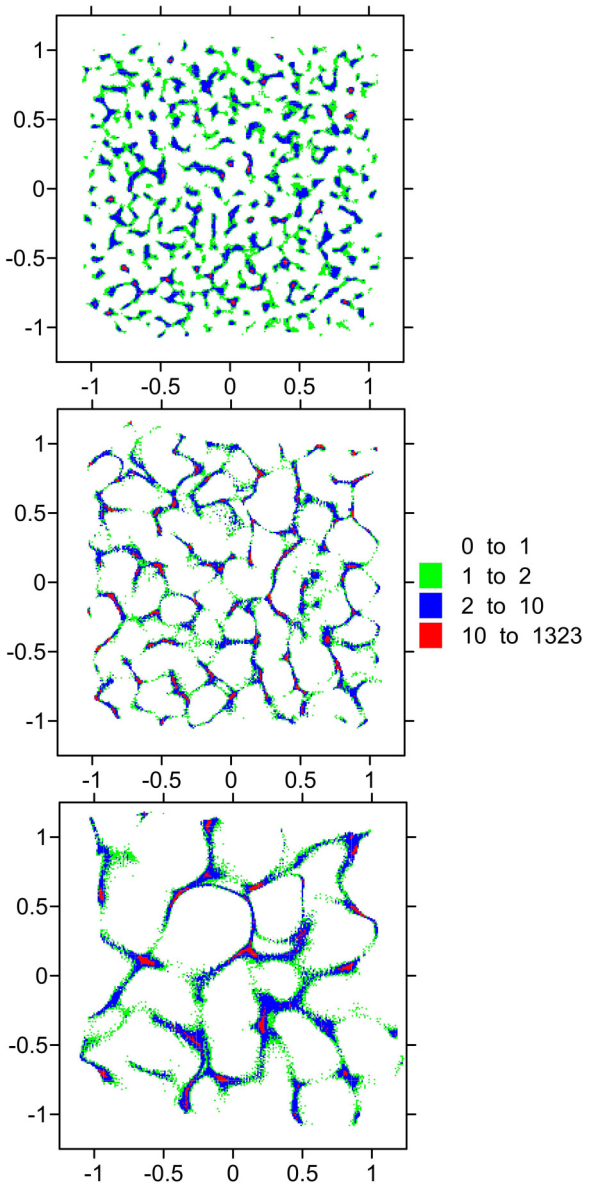

FIG. 2. The density distribution at the time $t = \tau$ for the parameters of the velocity field: $l = 0.04$, $\sigma_{\mathbf{u}} = 0.333$ (top), $l = 0.08$, $\sigma_{\mathbf{u}} = 0.666$ (center), $l = 0.16$, $\sigma_{\mathbf{u}} = 0.666$ (bottom).

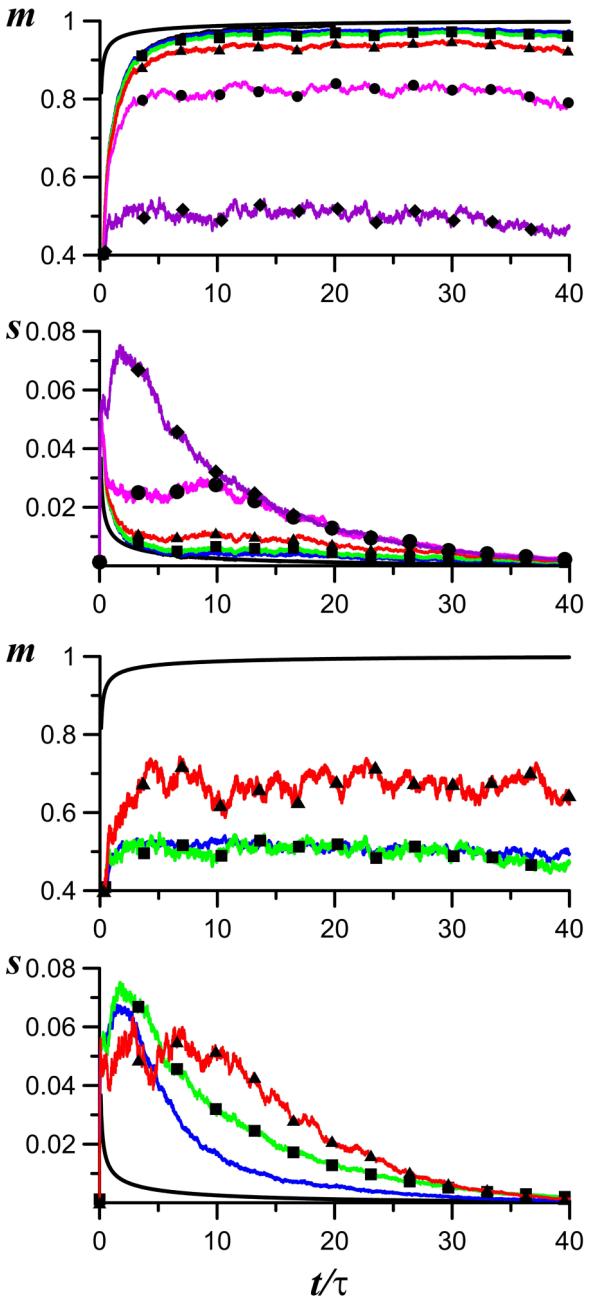

FIG. 3. The area and mass of all the clusters for $\bar{\rho} = 2.0$. (Top) $l = 0.08$, $\sigma_{\mathbf{u}} = 0.333$. The diffusion coefficients: $\kappa = 2 \times 10^{-4}$, marked by rhombus (purple); $\kappa = 2 \times 10^{-5}$, marked by circles (magenta); $\kappa = 2 \times 10^{-6}$, marked by triangles (red); $\kappa = 2 \times 10^{-7}$, marked by squares (green); $\kappa = 2 \times 10^{-8}$, not marked (blue). The curves with a greater value of κ are higher for the area and lower for the mass. (Bottom) The diffusion coefficient is $\kappa = 2 \times 10^{-4}$. The parameters of the velocity field are $l = 0.04$, $\sigma_{\mathbf{u}} = 0.333$, not marked (blue); $l = 0.08$, $\sigma_{\mathbf{u}} = 0.333$, marked by squares (green); $l = 0.16$, $\sigma_{\mathbf{u}} = 0.666$, marked by triangles (red). The bold lines correspond to the asymptotic values (9), (10).

where l is the space correlation radius and for effective diffusion coefficient (4), one can obtain expression

$$D = \frac{\sigma_{\mathbf{U}}{}^2}{l^2} t_0.$$

The equation (2) is numerically solved by means of a Monte Carlo simulation [10,22–24]. To that end, we consider an auxiliary field $\tilde{\rho}(\mathbf{R},t)$ governed by the stochastic equation

$$\frac{\partial}{\partial t}\tilde{\rho}(\mathbf{R},t) + \frac{\partial}{\partial \mathbf{R}}\mathbf{U}(\mathbf{R},t)\tilde{\rho}(\mathbf{R},t) = -\boldsymbol{\gamma}(t)\frac{\partial}{\partial \mathbf{R}}\tilde{\rho}(\mathbf{R},t), \quad (12)$$

with the initial condition $\tilde{\rho}(\mathbf{R},0) = \rho_0(\mathbf{R})$, and $\boldsymbol{\gamma}(t)$ being a δ-correlated Gaussian vector process independent of random velocity field $\mathbf{U}(\mathbf{R},t)$ such that $\langle \boldsymbol{\gamma}(t) \rangle = 0$, $\langle \gamma_\alpha(t)\gamma_\beta(t') \rangle = 2\kappa\delta_{\alpha\beta}\delta(t-t')$. A solution of Eq. (2), thus, corresponds to a solution of Eq. (12) averaged over the realization ensemble of $\boldsymbol{\gamma}(t)$ [10]

$$\rho(\mathbf{r},t) = \langle \tilde{\rho}(\mathbf{r},t) \rangle_{\boldsymbol{\gamma}(t)}.$$

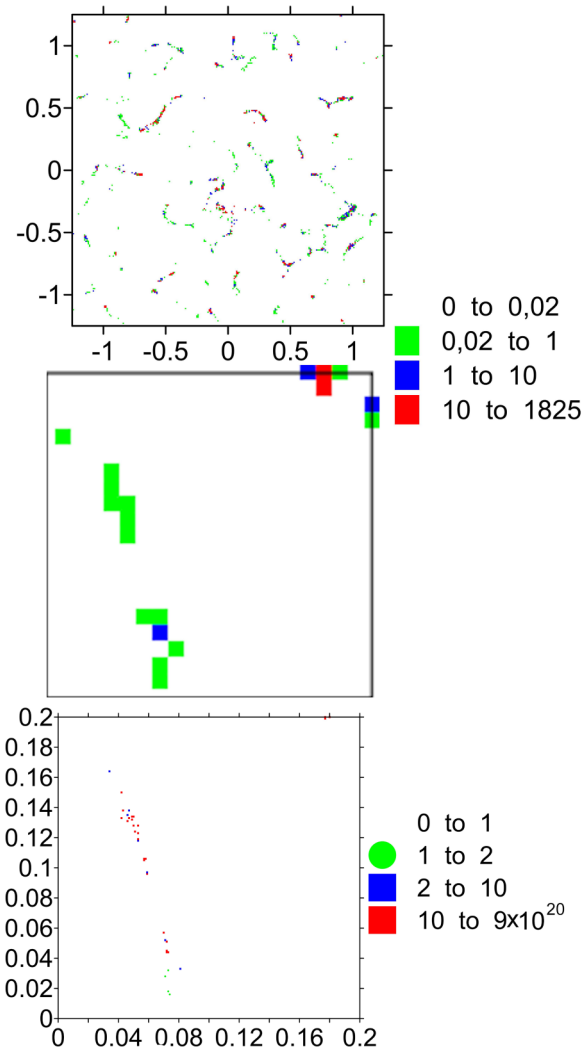

FIG. 4. The density distribution at the time $t = 27.3\tau$ for $l = 0.08$, $\sigma_{\mathbf{u}} = 0.333$,$\kappa = 0$ (top). The enlarged part (0/0.2, 0/0.2) (center). The same part calculated for a finer resolution in the space (bottom).

The equation (12) is solved by the characteristic method

$$\frac{d\mathbf{R}}{dt} = \mathbf{U}(\mathbf{R},t) + \boldsymbol{\gamma}(t), \quad \mathbf{R}(0) = \boldsymbol{\xi},$$
$$\frac{d\rho}{dt} = -\frac{\partial \mathbf{U}(\mathbf{R},t)}{\partial \mathbf{R}}\tilde{\rho}(t), \quad \tilde{\rho}(0) = \rho_0(\boldsymbol{\xi}). \tag{13}$$

The governing equations (13) are written in terms of the Lagrangian point of view. To turn into the Eulerian point of view, one can rewrite the solution of (13) in the form $\mathbf{R}(t) = \mathbf{R}(t;\boldsymbol{\xi}), \tilde{\rho}(t) = \tilde{\rho}(t;\boldsymbol{\xi})$. Now, by eliminating $\boldsymbol{\xi}$, one obtains the Eulerian definition of the density field $\rho(\mathbf{R},t) = \langle\tilde{\rho}(t)\rangle_{\boldsymbol{\gamma}} = \langle\tilde{\rho}[t;\boldsymbol{\xi}(\mathbf{R};t)]\rangle_{\boldsymbol{\gamma}}$. We will further address only the Eulerian representation of the density field.

B. Numerical results

To start, we consider the clustering process for $\kappa = 0$. Figure 1 shows the specific area and mass of the clusters depending on the time for $\bar{\rho} = 2.0$. The figures suggest that the area of all the clusters and their mass tends swiftly to the asymptotic values (9), (10) even in separate realizations. The curves appear similar given different values of the variance and space correlation radius. It is worth noticing that given small correlation radius values, the theoretical curves are attained slowly.

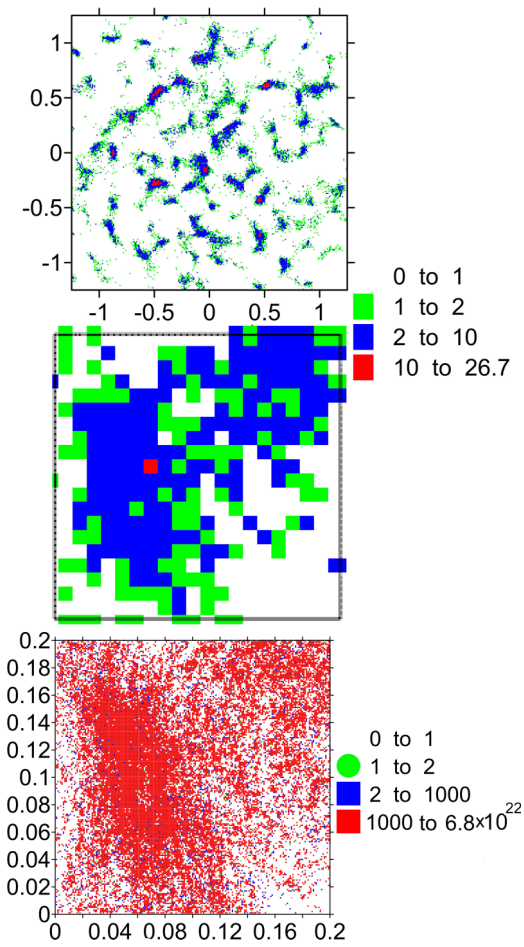

FIG. 5. The density distribution at the time $t = 27.3\tau$ for $l = 0.08$, $\sigma_{\mathbf{u}} = 0.333$, and $\kappa = 2 \times 10^{-4}$ (top). The enlarged part (0/0.2, 0/0.2) (center). The same part calculated for a finer resolution in the space (bottom).

Figure 2 shows that the empty regions among the clusters have a characteristic linear scale proportional to the space correlation radius. This result follows strictly from the numerical modeling and cannot be obtained analytically.

From common knowledge, one can assume that the diffusion is to force the cluster area to grow and the mass to shrink because of blurred cluster boundaries. However, the tracers emanated from a cluster may again converge into a new cluster. The intrinsic balance between these two processes determines the clustering dynamics. Figure 3 demonstrates that, at the initial stage, the clustering has no significant differences from the case of no diffusion. When the clusters approach the size of the diffusion scale, however, their area ceases to increase because of the diffusion. Then, the secondary clustering occurs in the diffused primary clusters. Hence, their area exponentially decreases. Contrary to the area, the mass of impurity concentrated in the clusters does not tend to the total mass of the tracers. From this, one can infer that the diffusion

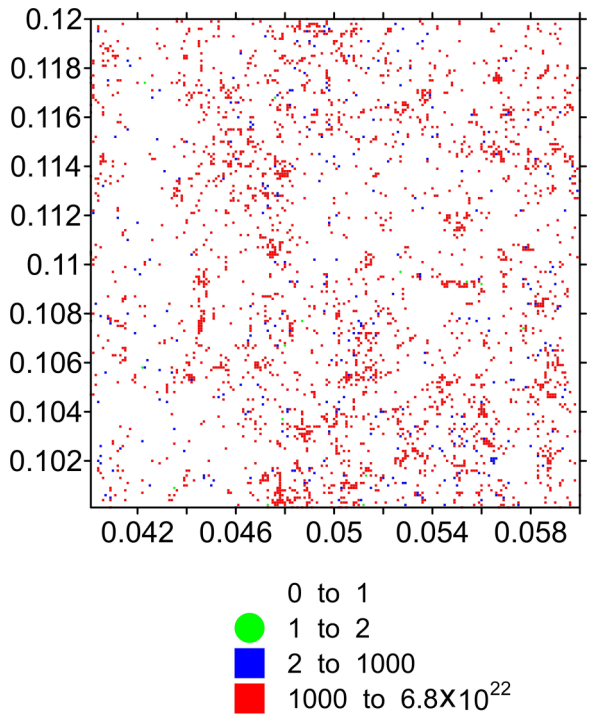

FIG. 6. The same as in the bottom panel of Fig. 5 for a range (0.04/0.06, 0.1/0.12) with a finer resolution.

do not terminate the clustering, but hinders it and results in that only a part of the impurity ends up in clusters.

The top panel of Fig. 3 illustrates the joint effect of the space correlation radius and diffusion. The figure indicates that as the correlation radius increases, the blurring due to diffusion is delayed. Given large values of the correlation radius, the number of tracers located in clusters increases.

Such a clustering process is to result in the cluster structure changing. Instead of one cluster, there is to appear a few smaller clusters within the areas comparative to the diffusion scale. Similar phenomenon has been reported for waves in random media where diffraction plays the role of the diffusion [13,14]. This phenomenon is called the contour splitting.

Figures 4 and 5 depict examples of the density distribution at the given time. It is worth noticing that a point in the figures comprising a cluster has a significantly higher area that the one of the cluster itself. Nevertheless, Fig. 4 attests that provided a finer resolution, the number of points comprising clusters changes very little. On the other hand, Fig. 5 demonstrates that given a finer resolution, a finer structure of clusters starts appearing. It is also worth mentioning that the density in the clusters, whose number increases once taking into account the diffusion, also significantly grows. The maximal density in a cluster attains 10^{20} in Fig. 4, and 10^{22} in Fig. 5. Comparing the bottom panel in Figs. 4 and 5, one can see that the markers cluster effectively within the diffusion scale near the vanished initial cluster.

The comparison of bottom panel of the Fig. 5 and the Fig. 6 illustrates the strong clustering below the diffusion scale near the initial cluster more clearly.

V. CONCLUSION

In this paper, we show that the diffusion effect is negligible at the initial stage for a uniform tracer distribution. In this case, clusters form in accordance with the asymptotic relations (9), (10). The characteristic size of the regions with small impurity concentration is shown to be proportional to the space correlation radius of the velocity field. In the presence of the diffusion, clusters always form. However, the clusters disintegrate engendering new smaller clusters. These new clusters are concentrated within the regions of the diffusion scale near the initial cluster. It is worth noting that the cluster splitting due to the diffusion becomes apparent only after longer integration times. Because of this fact, the effect was not revealed earlier in the work [22], where, first, an insufficient integration time and, second, a coarse space resolution were implemented.

As a concluding remark, we note that an analogous effect of contour splitting was reported for a stochastic problem of laser emission in random media [13,14]. The problem was formulated by means of Leontovich equation (Schrödinger equation) with the diffraction playing the role of the diffusion. The contour splitting, described analytically by means of reformulating the problem in terms of the continual integral, allows us to interpret the numerical results reported in this paper in particular and various calculation and experimental data in general.

ACKNOWLEDGMENTS

The analytical estimates carried out by V. I. Klyatskin was supported by the Russian Science Foundation, Project No. 14-27-00134. Numerical modeling carried out by K. V. Koshel was supported by the Russian Science Foundation, Project No. 16-17-10025.

[1] A. Okubo, *Diffusion and Ecological Problems: Mathematical Models*, Biomathematics Vol. 10 (Springer-Verlag, Berlin, 1980).

[2] W. D. Mc Comb, *The Physics of Fluid Turbulence*, Oxford Engineering Science Series Vol. 25 (Clarendon Press, Oxford, 1990).

[3] G. A. Jacobs, H. S. Huntley, A. D. Kirwan, B. L. Lipphardt, T. Campbell, T. Smith, K. Edwards, and B. Bartels, J. Geophys. Res. Oceans **121**, 180 (2016).

[4] K. L. Law, S. Morét-Ferguson, N. A. Maximenko, G. Proskurowski, E. E. Peacock, J. Hafner, and C. M. Reddy, Science **329**, 1185 (2010).

[5] A. Cozar, F. Echevarria, J. I. Gonzalez-Gordillo, X. Irigoien, B. Ubeda, S. Hernandez-Leon, A. T. Palma, S. Navarro, J. Garcia-de-Lomas, A. Ruiz, M. L. Fernandez-de-Puelles, and C. M. Duarte, Proc. Natl. Acad. Sci. **111**, 10239 (2014).

[6] A. Kostinski and R. Shaw, J. Fluid Mech. **434**, 389 (2001).

[7] G. Dagan, Annu. Rev. Fluid Mech. **19**, 183 (1987).

[8] I. de Pater and J. Lissauer, *Planetary Science* (Cambridge University Press, Cambridgew, 2001).
[9] S. F. Shandarin and Ya. B. Zeldovich, Rev. Mod. Phys. **61**, 185 (1989).
[10] V. I. Klyatskin, Phys. Usp. **37**, 501 (1994).
[11] R. Monchaux, M. Bourgoin, and A. Cartellier, Phys. Fluids **22**, 103304 (2010).
[12] M. Bourgoin and H. Xu, New J. Phys. **16**, 085010 (2014).
[13] V. I. Klyatskin, *Stochastic Equations: Theory and Applications in Acoustics, Hydrodynamics, Magnetohydrodynamics, and Radiophysics*, Vols. 1, 2 (Springer, Berlin, 2015).
[14] V. I. Klyatskin, Phys. Usp. **59**, 67 (2016).
[15] V. I. Klyatskin and A. I. Saichev, JETP **84**, 716 (1997).
[16] G. Boffetta, J. Davoudi, B. Eckhardt, and J. Schumacher, Phys. Rev. Lett. **93**, 134501 (2004).
[17] M. Maxey, J. Fluid Mech. **174**, 441 (1987).
[18] V. I. Klyatskin, Phys. Usp. **46**, 667 (2003).
[19] V. I. Klyatskin, JETP **99**, 1005 (2004).
[20] J. R. Cressman and W. I. Goldburg, J. Stat. Phys. **113**, 875 (2003).
[21] P. Gutierrez and S. Aumaitre, Eur. J. Mech. B Fluid. **60**, 24 (2016).
[22] K. V. Koshel' and O. V. Aleksandrova, Izv. Atmos. Ocean. Phys. **35**, 578 (1999).
[23] U. Frisch, A. Mazzino, and M. Vergassola, Phys. Rev. Lett. **80**, 5532 (1998).
[24] Omri Gat, Itamar Procaccia, and Reuven Zeitak, Phys. Rev. Lett. **80**, 5536 (1998).
[25] J. R. Cressman, J. Davoudi, W. I. Goldburg, and J. Schumacher, New J. Phys. **6**, 53 (2004).
[26] J. Larkin, W. Goldburg, and M. M. Bandi, Physica D **239**, 1264 (2010).
[27] S. Lovecchio, C. Marchioli, and A. Soldati, Phys. Rev. E **88**, 033003 (2013).
[28] V. I. Klyatskin and D. Gurarie, Phys. Usp. **42**, 165 (1999).
[29] M. B. Isichenko, Rev. Mod. Phys. **64**, 961 (1992).
[30] Craig L. Zirbel and Erhan Cinlar, in *Stochastic Models in Geosystems*, IMA Volumes in Mathematics and its Applications (Springer-Ver1ag, New York, 1996).
[31] A. P. Roberts and M. Teubner, Phys. Rev. E **51**, 4141 (1995).